NACA

RESEARCH MEMORANDUM

FLIGHT MEASUREMENTS AT MACH NUMBERS FROM 1.1 TO 1.9

OF THE ZERO-LIFT DRAG OF A TWIN-ENGINE

SUPERSONIC RAM-JET CONFIGURATION

By Abraham Leiss

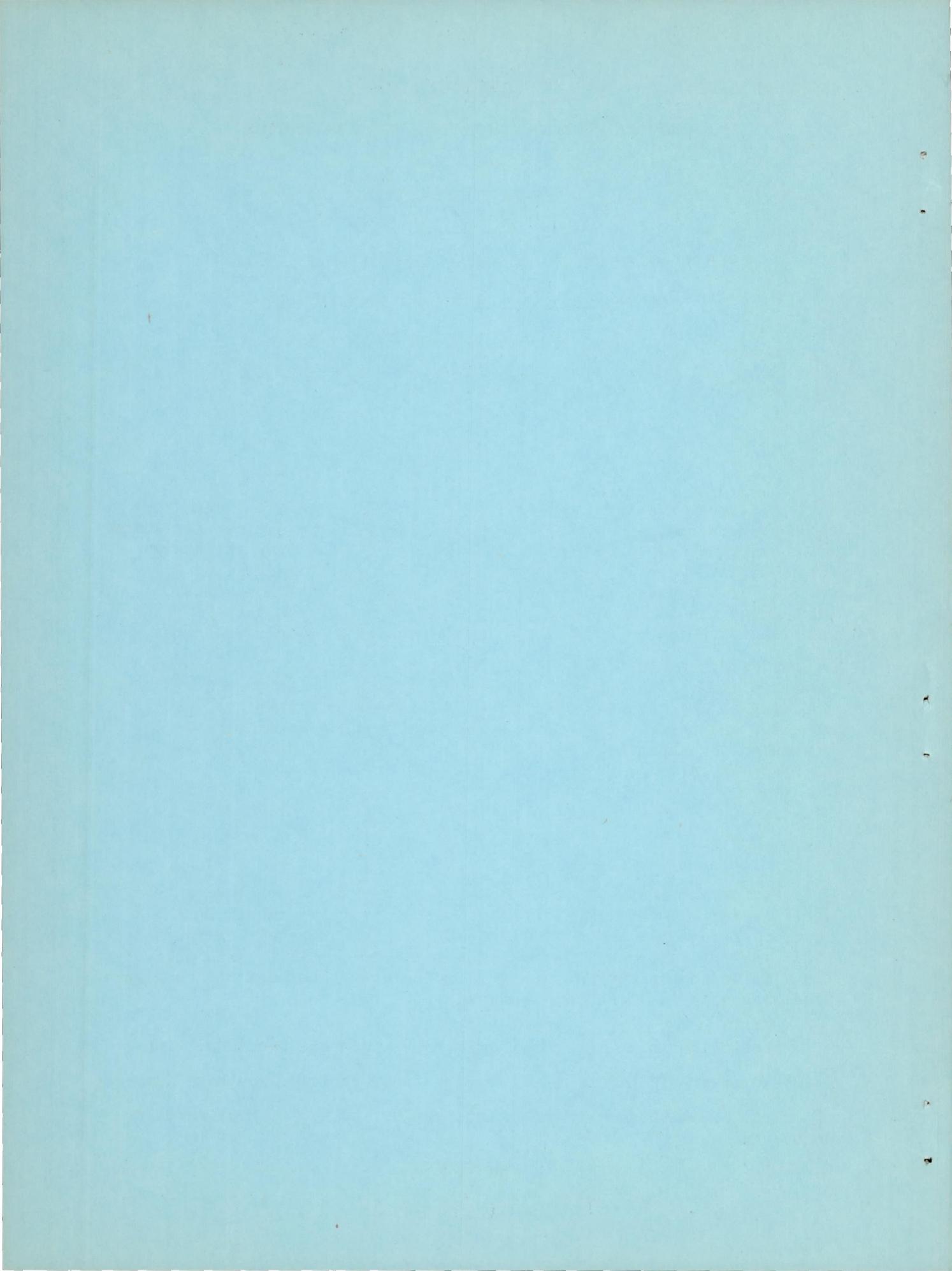Langley Aeronautical Laboratory
Langley Field, Va.

CLASSIFICATION CHANGED TO UNCLASSIFIED
AUTHORITY: RESEARCH ABSTRACT NO. 101
DATE: MAY 25, 1956   WHL

NATIONAL ADVISORY COMMITTEE
FOR AERONAUTICS
WASHINGTON
June 23, 1952

NATIONAL ADVISORY COMMITTEE FOR AERONAUTICS

———————

RESEARCH MEMORANDUM

———————

FLIGHT MEASUREMENTS AT MACH NUMBERS FROM 1.1 TO 1.9

OF THE ZERO-LIFT DRAG OF A TWIN-ENGINE

SUPERSONIC RAM-JET CONFIGURATION

By Abraham Leiss

SUMMARY

A flight investigation was conducted to determine the zero-lift drag characteristics of a twin-engine supersonic ram-jet configuration, which were needed to make performance calculations below the design Mach number. Data were obtained over a Mach number range from 1.1 to 1.9 for two power-off ram-jet models - with and without nacelles - to supplement the performance data obtained from previous tests at higher supersonic speeds. The Reynolds number, based on fuselage length,

ranged from 53×10^6 at a Mach number of 1.1 to 118×10^6 at a Mach number of 1.9. The external drag of the nacelle units, which included the drag of the inboard wedge-type struts, outboard fairings, and nacelles and their mutual interference drag, was determined and accounted for approximately 60 percent of the total external drag of this configuration.

INTRODUCTION

Performance data from the flight test of a ram-jet-powered test vehicle (ref. 1) were obtained over a range of Mach numbers from 1.8 to 2.6. An analysis of the performance data of this twin-engine supersonic ram-jet test vehicle led to the need for zero-lift drag data of the missile component parts as well as the need to extend the configuration drag data to lower Mach numbers.

Free-flight zero-lift drag tests have therefore been made with $\frac{5}{8}$-scale power-off models of the ram-jet test vehicle from Mach numbers of 1.1 to 1.9 with nacelle units and from 0.7 to 2.0 without nacelle units.

The total and component drag coefficients of the two models tested
for a Reynolds number range of 20×10^6 to 118×10^6 are presented in
this paper. The Reynolds number was based on the body length (9.87 feet).

SYMBOLS

A   maximum fuselage cross-sectional area

A_b nacelle exit area

A_t tail-plug area

C_D drag coefficient, $D/q_0 A$

D   drag

D_b base drag, $A_t(p_0 - p_b)$

M   flight Mach number

p   static pressure

p_b base pressure in tail plug

p_0 free-stream static pressure

P   pressure coefficient, $\dfrac{p - p_0}{q_0}$

q_0 free-stream dynamic pressure

r   radius of fuselage

R   Reynolds number based on fuselage length (9.87 feet)

γ ratio of specific heats of air (1.40)

DESCRIPTION OF MODELS

Sketches and photographs of the models are shown in figures 1 to 5.
Both models had cone-cylinder-cone fuselages and were 118.46 inches long
with maximum fuselage diameters of 5 inches (fineness ratio 23.69).

Model A was a $\frac{5}{8}$-scale replica of the ram-jet test vehicle described in reference 1. As shown in figure 1, model B has the nacelle units removed and replaced by two additional fins.

Test configuration A had tail plugs installed inside its simulated engines. These tail plugs were designed to give sonic flow at the exit so that the air mass flow could be calculated and an accurate determination of the internal nacelle drag could be made. The internal nacelle drag data were then used to determine the external drag of test configuration A. The entrance area of the inlet was 3.56 square inches and the throat area, slightly downstream of the inlet lip, was 3.06 square inches. The exit area at the tail plug was 3.47 square inches.

INSTRUMENTATION AND FLIGHT TESTING

Model A was instrumented with a two-channel telemeter, which was used to measure longitudinal acceleration and nacelle-tail-plug base pressure by use of a single orifice. Model B was instrumented with the same type of two-channel telemeter but was used to measure longitudinal acceleration only.

Both models were boosted with 6.25-inch ABL Deacon rocket motors. Photographs of the models and boosters on the launching stand are shown as figure 5. After being accelerated to a Mach number of approximately 2.0, the models separated from the booster and zero-lift data were obtained during the coasting flight.

Velocity and Mach number of test vehicles A and B were obtained by the use of continuous-wave Doppler radar and by the integration of the data from the longitudinal accelerometers. The trajectories of the models were obtained by NACA modified SCR 584 tracking radar. Atmospheric data for each flight were obtained by means of a balloon carrying a radiosonde sent aloft at the time of each flight.

The estimated error of the experimental total drag coefficients is believed to be within the following limits:

Model A:
At Mach number 1.1 . . . . ± 0.024
At Mach number 1.9 . . . . ± 0.014

Model B:
At Mach number 0.8 . . . . ± 0.009
At Mach number 2.0 . . . . ± 0.008

The estimated error of the calculated external drag coefficients of Model A is believed to be within the following limits:

At Mach number 1.1 . . . . ±0.027
At Mach number 1.9 . . . . ±0.017

RESULTS AND DISCUSSION

The variation of Reynolds number with Mach number for each test configuration is shown in figure 6. Also shown is the Reynolds number of the test vehicle described in reference 1. The ratio of base pressure on the tail plug to free-stream static pressure, necessary in the determination of the nacelle-tail-plug base drag, is shown as a function of Mach number in figure 7. The sudden change in pressure ratio near Mach number 1.91 is probably due to booster separation. During boosted flight the proximity of the booster to the tail plug caused a local high-pressure region and influenced the tail-plug reading. It is interesting to note that, as the test vehicle decelerated from the supersonic to the subsonic velocities, a sharp rise in pressure ratio occurred.

Total and external drag coefficients (based on fuselage cross-sectional area) obtained from the flights of the models are presented in figure 8. The external drag coefficients for model A were obtained by subtracting the internal and tail-plug base drag from the model total drag. The internal nacelle drag was determined by calculating the change of pressure and momentum between the free stream and the exit (refs. 2 and 3).

Note in figure 8 that, although the Reynolds number for model A at a Mach number of 1.87 was about four times that for the full-scale test vehicle, the external-drag curves coincide. This unexpected agreement may be explained on the basis of a typical curve of drag plotted against Reynolds number, wherein the same drag coefficient may be obtained at three different Reynolds numbers, depending on whether the boundary layer is fully laminar, partially laminar and partially turbulent, or fully turbulent. The Reynolds number for model A indicates that the flow was probably fully turbulent. It is possible that the Reynolds number of the full-scale model resulted in partially laminar and partially turbulent boundary layer and was of just the value to produce the same drag coefficient. It is acknowledged that this explanation is only qualitative and probably incomplete because there are other possible causes.

Presented in figure 9 are the model-component drag coefficients. The theoretical pressure-drag coefficient of the fuselage was computed by integrating the pressure distribution determined by the method

described in reference 4. The friction-drag coefficients of the fuse-
lage were determined by the method described in reference 5. The sum
of the theoretical pressure and friction drags of the fuselage is shown
to be in close agreement with the experimental data presented in refer-
ence 6. By subtracting the fuselage drag from the total drag of model B,
the drag and interference attributed to four fins were determined. By
using half of this value the drag-coefficient curve for the fuselage
with two fins was determined. For comparative purposes the total drag
of model B and the external drag of model A have been replotted in fig-
ure 9. The difference between the external drag of model A and the drag
of the two-fin and fuselage configuration can be attributed to the
nacelle units and their mutual interferences (as shown in fig. 10).
The nacelle units, consisting of inboard wedge-type struts, ducted
nacelles, and outboard fairings, account for a large percentage of the
total external drag.

CONCLUDING REMARKS

Free-flight drag tests at zero lift have been made of a power-off
ram-jet model with nacelles and a similar model without nacelles. Drag
data were obtained from a Mach number range of 1.1 to 1.9 to supplement
the drag data already existing for higher supersonic speeds. The drag
of the nacelle units, consisting of the drag of inboard and outboard
wedge-type struts, nacelles, and outboard fairings and their associated
interference drag, was about 60 percent of the total external drag for
the Mach number range covered.

Langley Aeronautical Laboratory
    National Advisory Committee for Aeronautics
        Langley Field, Va.

REFERENCES

1. Faget, Maxime A., and Dettwyler, H. Rudolph: Initial Flight Investigation of a Twin-Engine Supersonic Ram Jet. NACA RM L50H10, 1950.

2. Faget, Maxime A., Watson, Raymond S., and Bartlett, Walter A., Jr.:
Free-Jet Tests of a 6.5-Inch-Diameter Ram-Jet Engine at Mach
Numbers of 1.81 and 2.00. NACA RM L50L06, 1951.

3. Dailey, C. L., McFarland, H. W., and DeVault, R. T.: Bi-Monthly
Progress Report for February, 1949 and March, 1949. Development
of Ramjet Components. Contract NOa(s) 9961. P.R. 9961-3, Navy
Res. Project, Univ. Southern Calif. Aero. Lab., Apr. 7, 1949.

4. Von Kármán, Theodor, and Moore, Norton B.: Resistance of Slender
Bodies Moving With Supersonic Velocities With Special Reference to
Projectiles. Trans. A.S.M.E., vol. 54, no. 23, Dec. 15, 1932,
pp. 303-310.

5. Van Driest, E. R.: Turbulent Boundary Layer for Compressible Fluids
on an Insulated Flat Plate. Rep. No. AL-958, North American
Aviation, Inc., Sept. 15, 1949.

6. Welsh, Clement J., and deMoraes, Carlos A.: Results of Flight Tests
To Determine Drag of Parabolic and Cone-Cylinder Bodies of Very
Large Fineness Ratios at Supersonic Speeds. NACA RM L51E18, 1951.
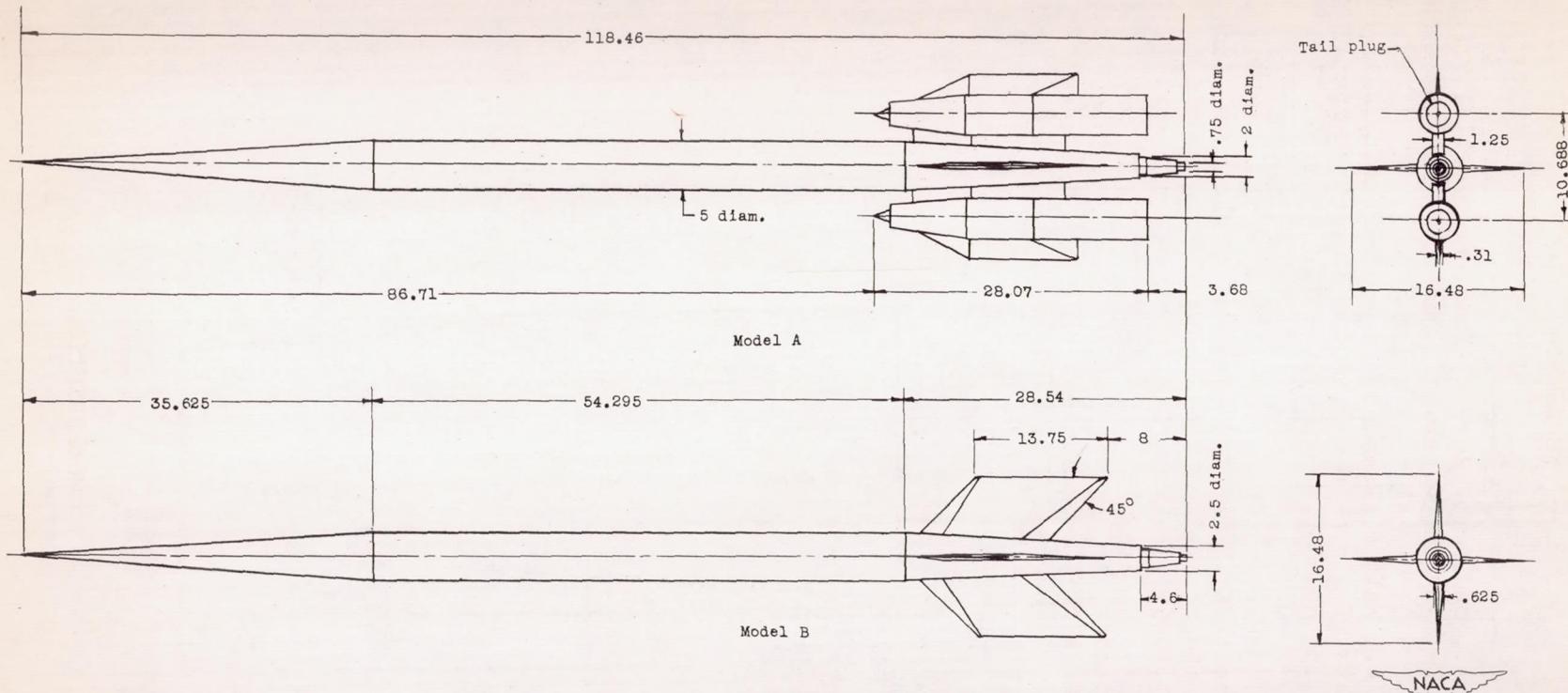
Figure 1.- General arrangement of cone-cylinder-cone test configurations.
All dimensions are in inches.

NACA RM L52D24

Section view of inboard strut
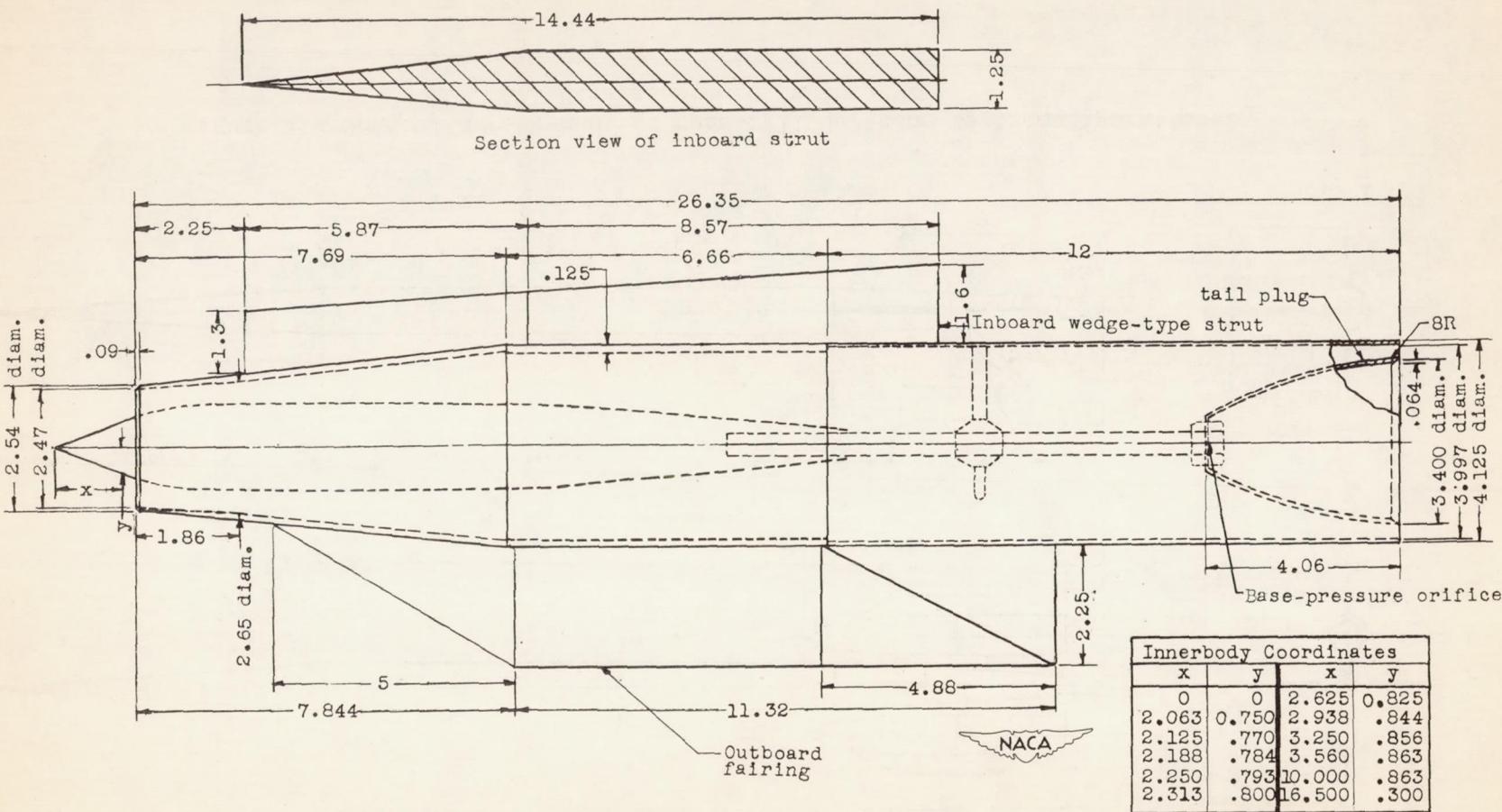
Figure 2.- Sketch showing internal geometry of nacelle. All dimensions
are in inches.

Innerbody Coordinates			
x	y	x	y
0	0	2.625	0.825
2.063	0.750	2.938	.844
2.125	.770	3.250	.856
2.188	.784	3.560	.863
2.250	.793	10.000	.863
2.313	.800	16.500	.300
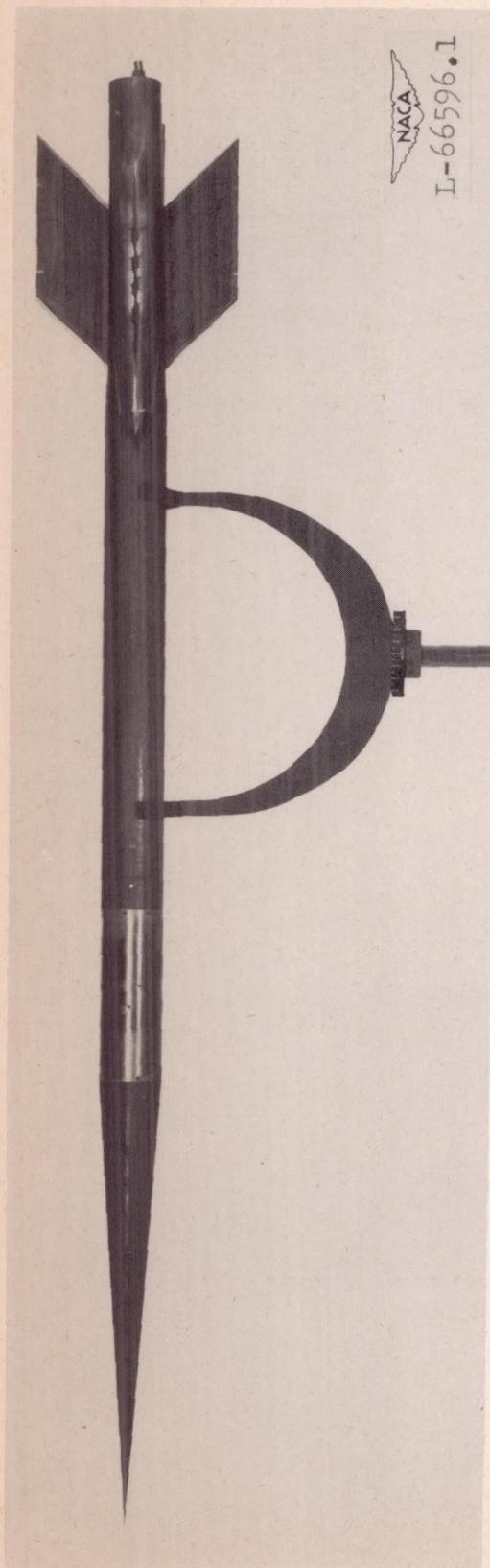
Side view
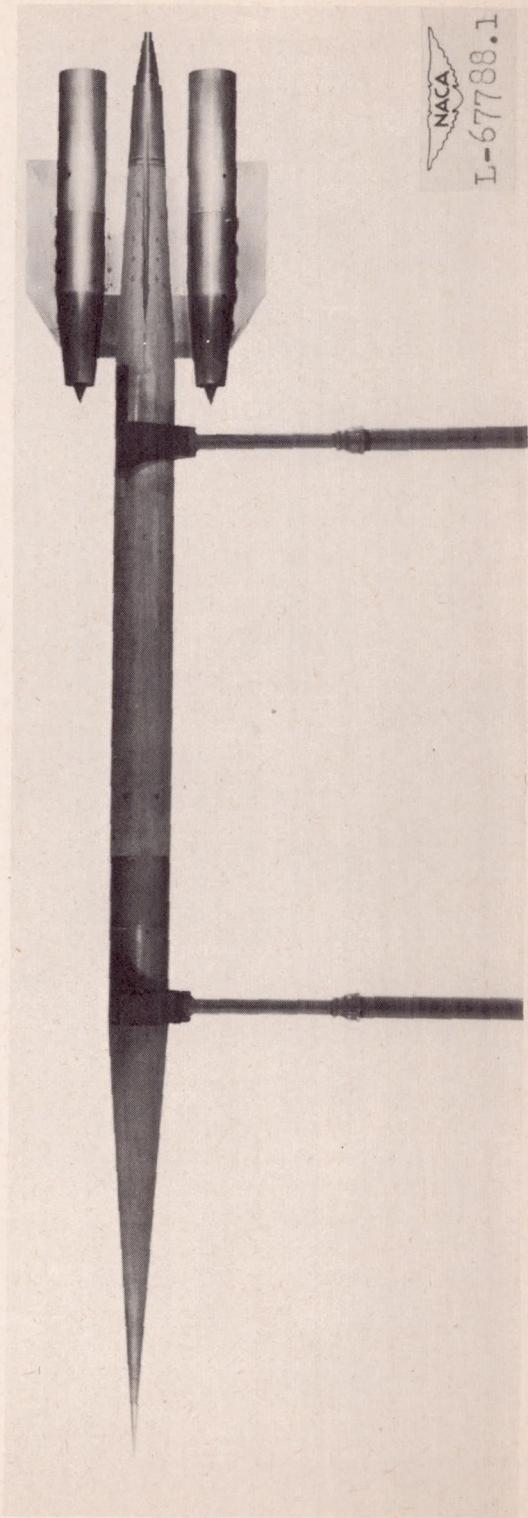
Plan view

Figure 3.- Model A.
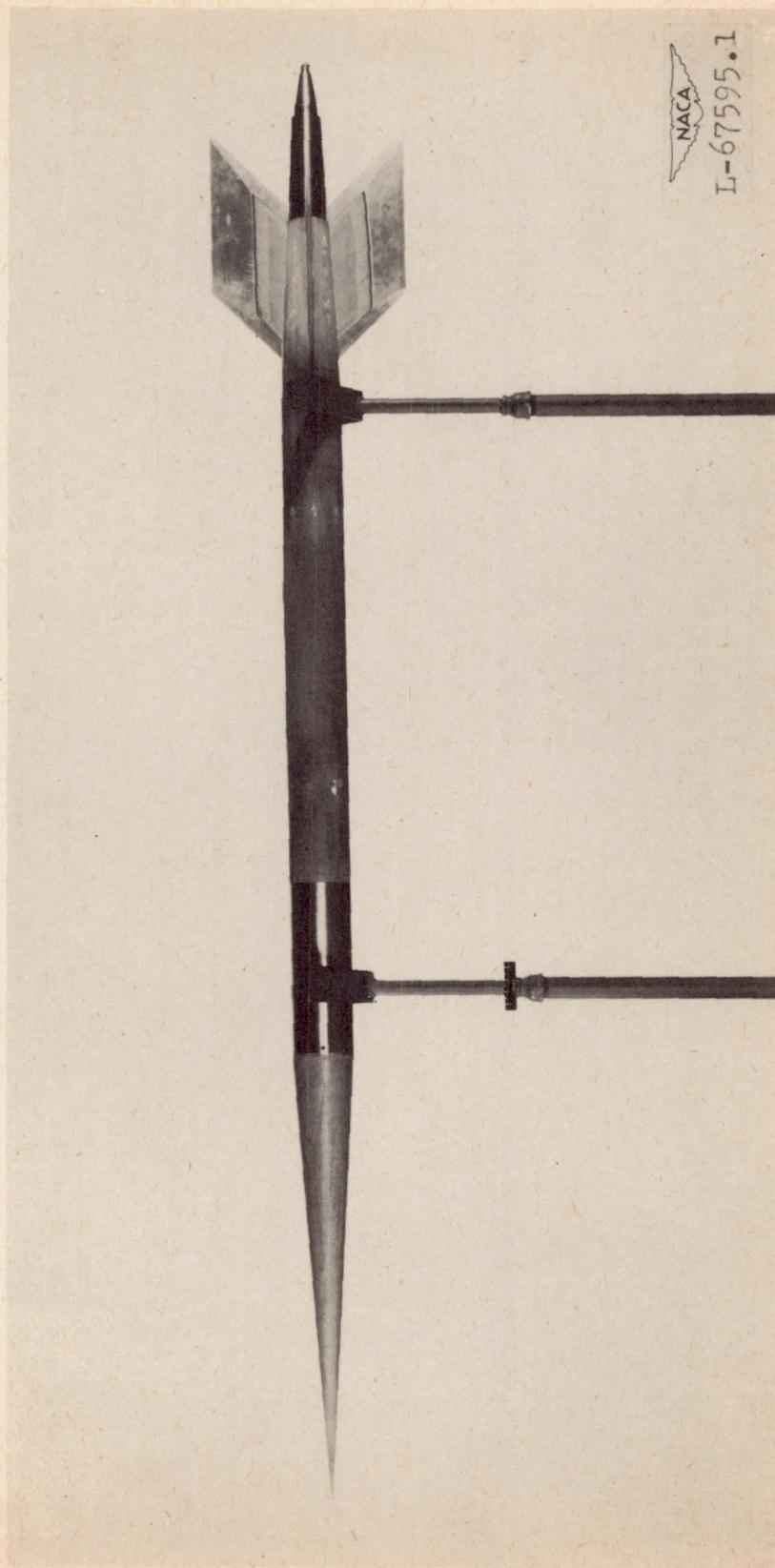
Figure 4.- Model B.
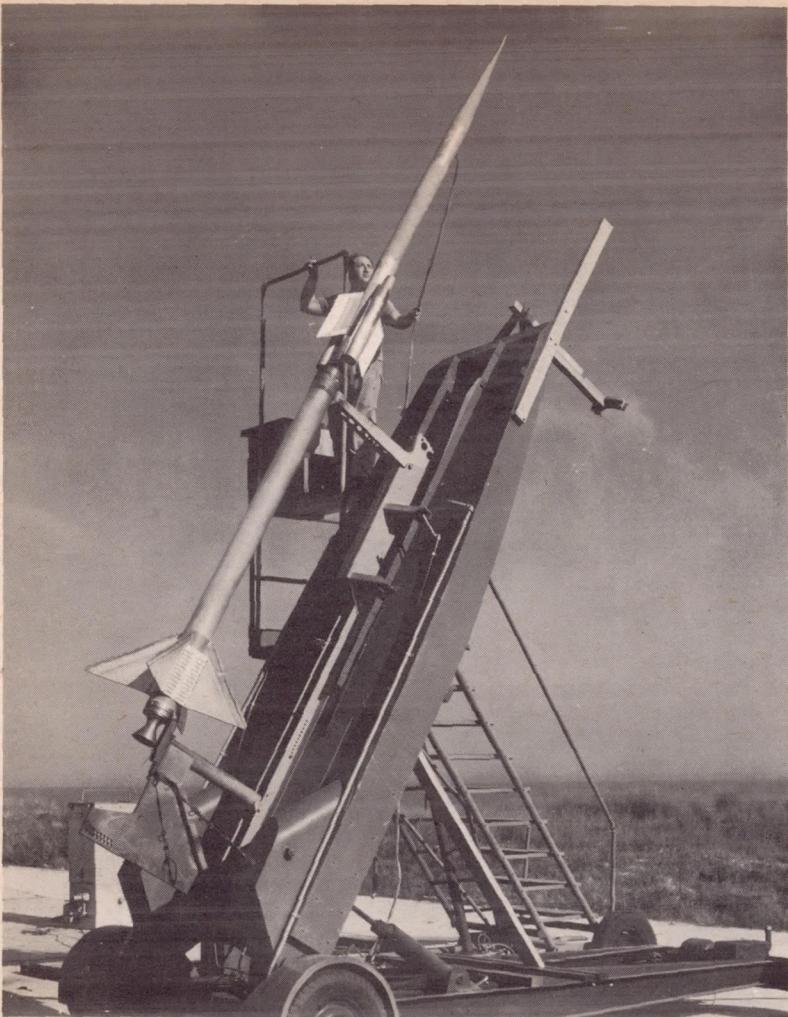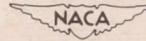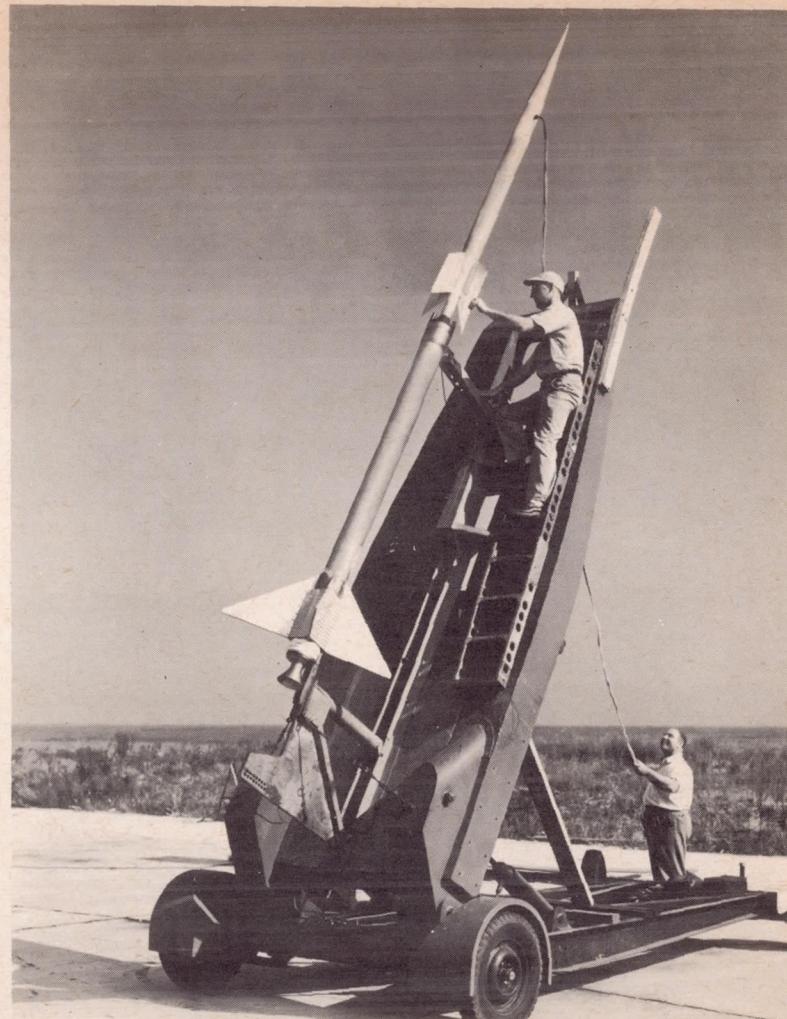
Model A   L-68052.1   Model B   L-67692.1
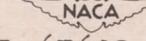
Figure 5.- Models elevated 60° on launcher.
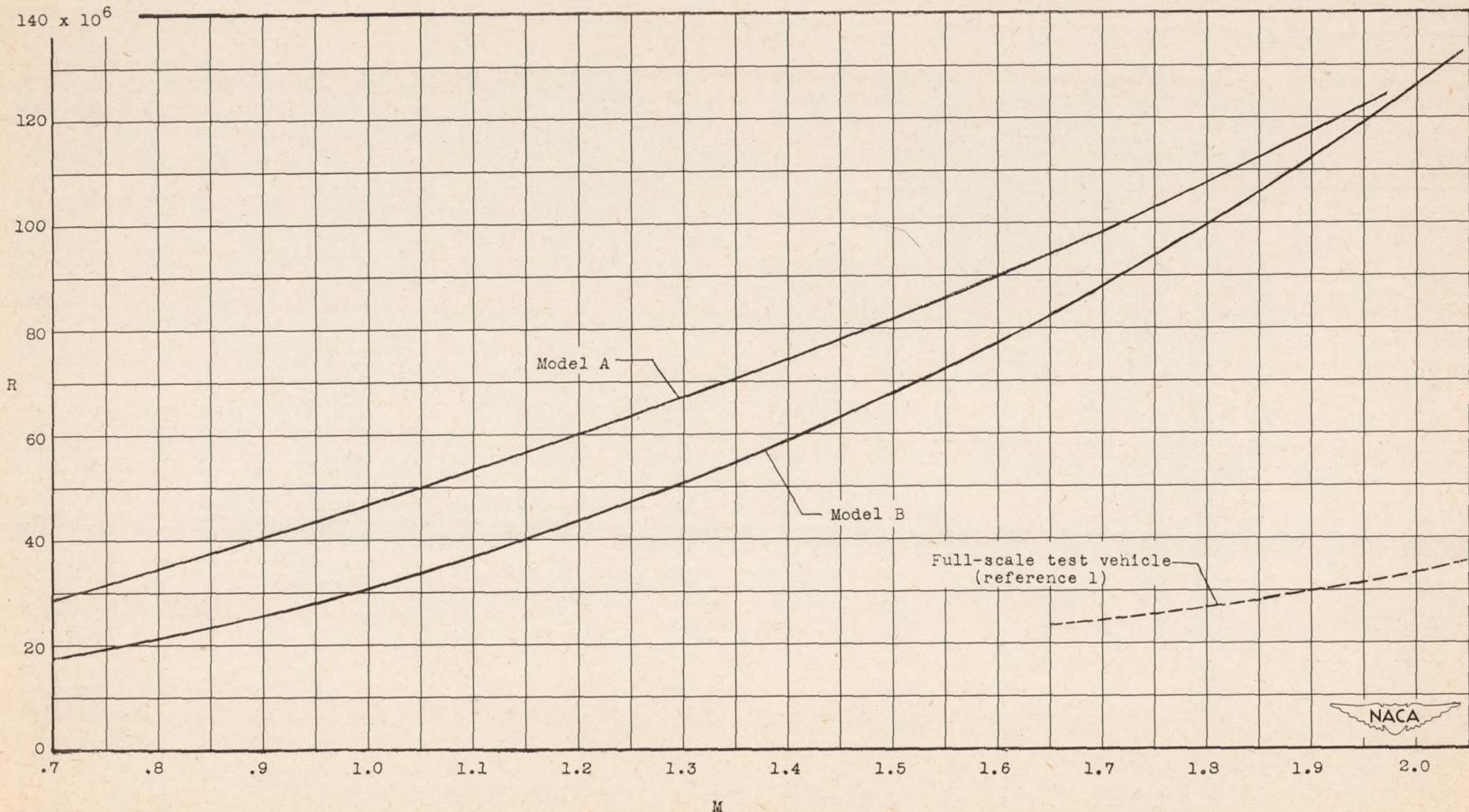
Figure 6.- Reynolds number (based on fuselage length, 9.87 ft) variation with Mach number.
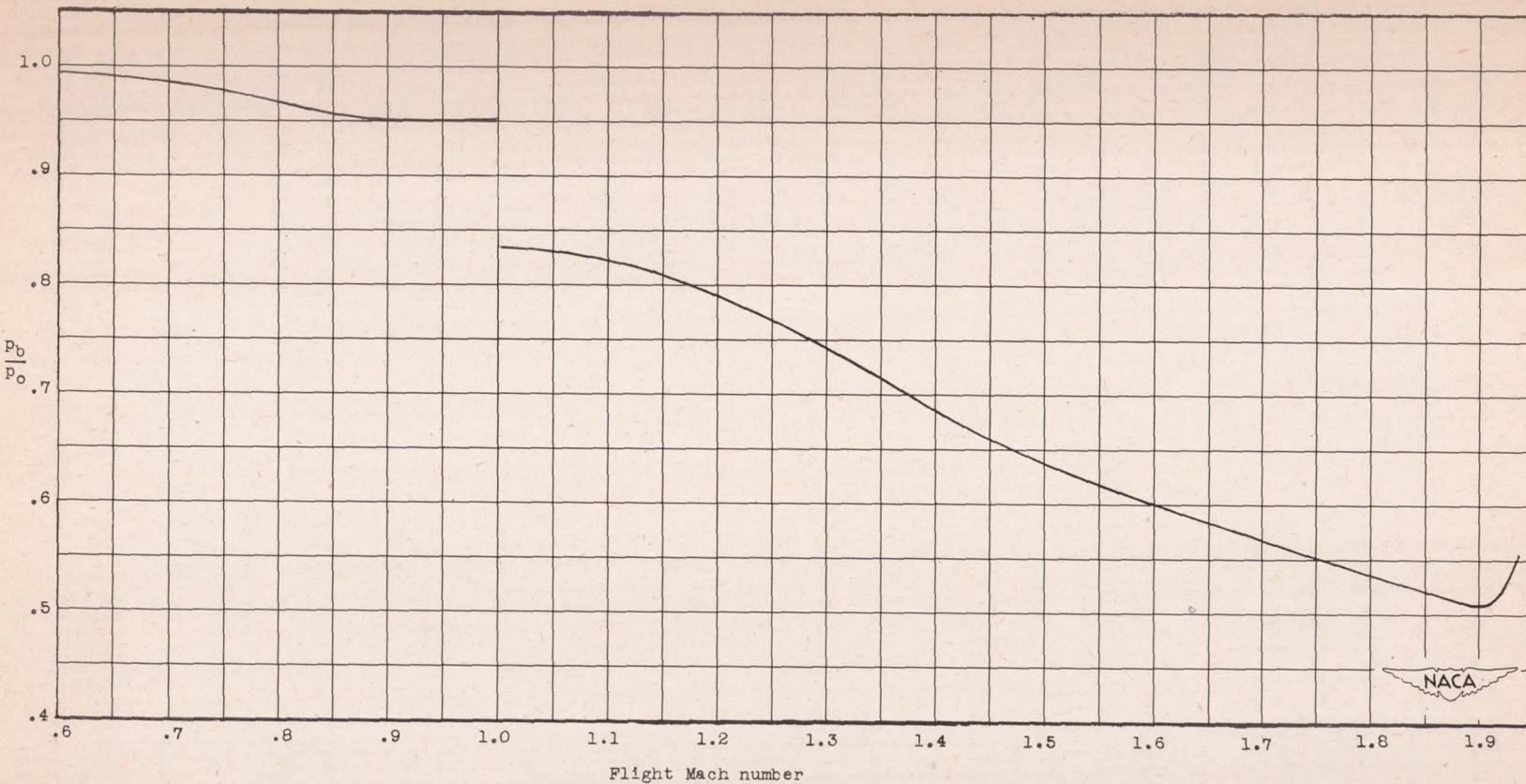
Figure 7.- Ratio of nacelle base pressure to free-stream static-pressure
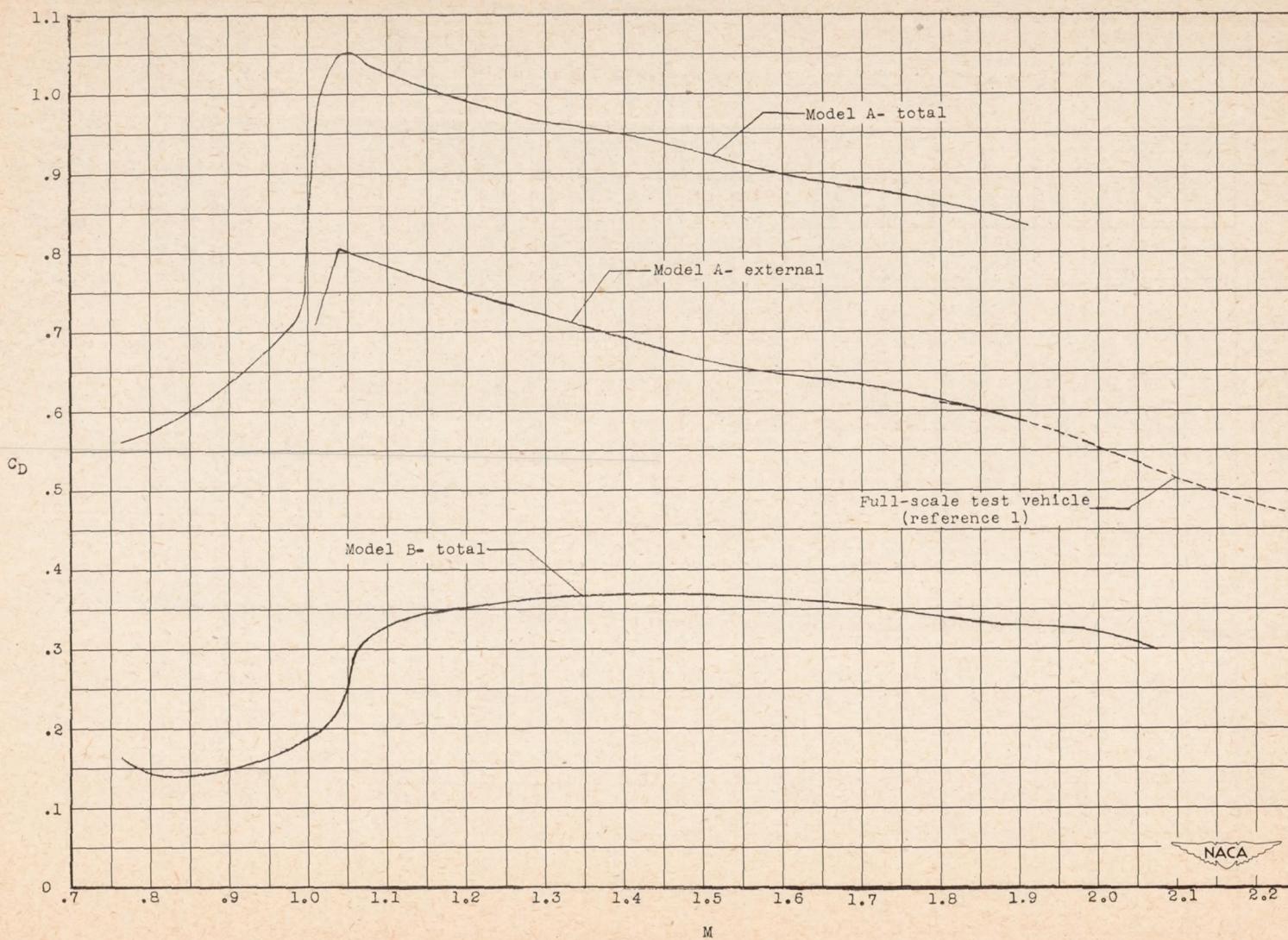variation with Mach number for model A.

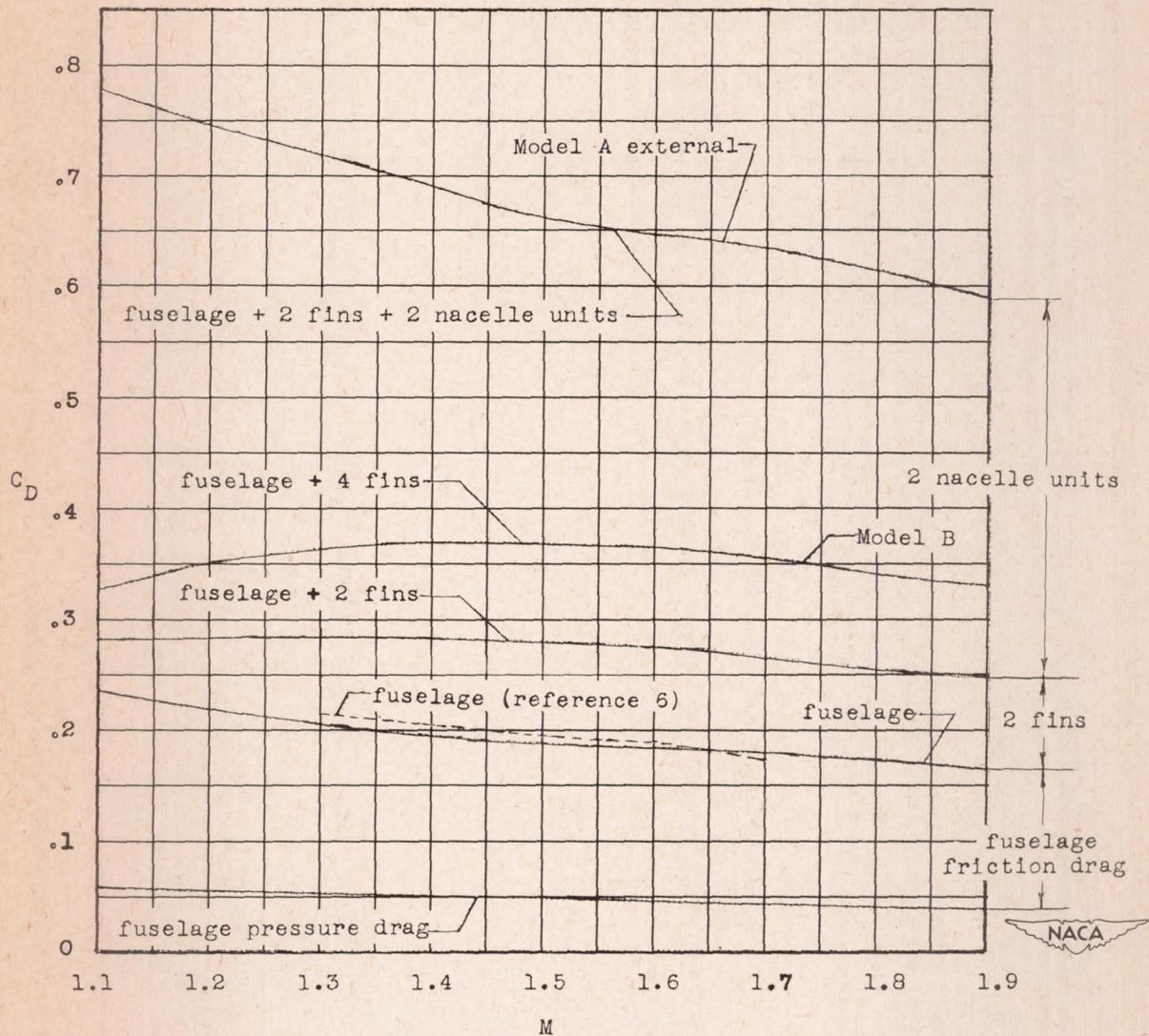Figure 8.- Variations of drag coefficients with Mach number.

Figure 9.- Variation of experimental and theoretical drag coefficients
with Mach number for the component parts of the models tested.
Note: Nacelle-unit drag consists of inboard-strut drag, outboard-
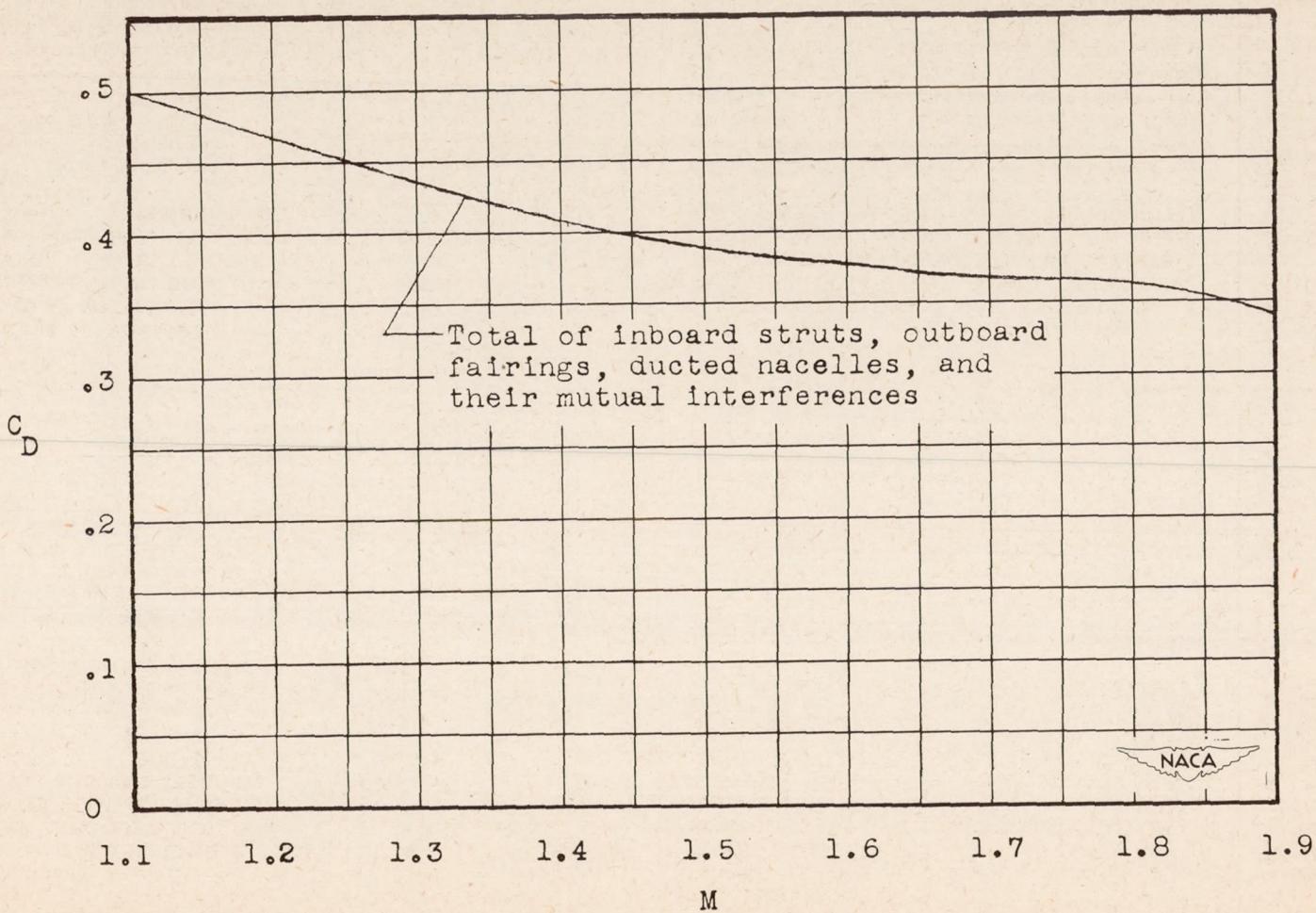fairing drag, ducted-nacelle drag, and mutual interference drags.

Figure 10.- Variation of drag coefficients with Mach number for nacelle units.